New Phytologist

PHOTOSYNTHESIS ACROSS AFRICAN CASSAVA GERMPLASM IS LIMITED BY RUBISCO AND MESOPHYLL CONDUCTANCE AT STEADY-STATE, BUT BY STOMATAL CONDUCTANCE IN FLUCTUATING LIGHT

Journal:	*New Phytologist*
Manuscript ID	NPH-MS-2019-29950
Manuscript Type:	MS - Regular Manuscript
Date Submitted by the Author:	24-Apr-2019
Complete List of Authors:	De Souza, Amanda; University of Illinois at Urbana-Champaign, Carl R. Woese Institute for Genomic Biology Wang, Yu; University of Illinois, Institute for Genomic Biology Orr, Douglas; Lancaster University, Lancaster Environment Centre Carmo-Silva, Elizabete ; University of Lancaster , Lancaster Environment Centre Long, Stephen; University of Illinois, Institute for Genomic Biology
Key Words:	cassava, crop breeding, food security, bioengineering, Manihot esculenta, photosynthesis, Rubisco, water use efficiency

PHOTOSYNTHESIS ACROSS AFRICAN CASSAVA GERMPLASM IS LIMITED BY RUBISCO AND MESOPHYLL CONDUCTANCE AT STEADY-STATE, BUT BY STOMATAL CONDUCTANCE IN FLUCTUATING LIGHT

Amanda P. De Souza[1], Yu Wang[1], Douglas J. Orr[2], Elizabete Carmo-Silva[2], Stephen P. Long[1,2*]

[1] Carl R Woese Institute for Genomic Biology, University of Illinois at Urbana-Champaign, Urbana, IL, 61801, USA

[2] Lancaster Environment Centre, Lancaster University, Lancaster, LA1 4YQ, UK

[*] Corresponding author: slong@illinois.edu

Total word count (excluding summary, references and legends): 6523

Summary: 200

Introduction: 1163

Material and Methods: 2048

Results: 1476

Discussion: 1749

Acknowledgements: 86

Number of Figures: 6

Number of Tables: 2

Number of Supporting Information Files: 1

SUMMARY

- Sub-Saharan Africa is projected to see a 55% increase in food demand by 2035, where cassava (*Manihot esculenta*) is the most planted crop and a major calorie source. Cassava yield has not increased significantly for 13 years. Improvement of genetic yield potential, the basis of the first Green Revolution, can be increased by improving photosynthetic efficiency. First, the factors limiting photosynthesis and genetic variability in these within extant germplasm must be understood.
- We analyzed biochemical and diffusive limitations to leaf photosynthetic CO_2 uptake under steady-state and fluctuating light in thirteen farm-preferred and high-yielding African cultivars. We developed a cassava leaf metabolic model to quantify the value of overcoming limitations at different points in photosynthesis.
- At steady-state, *in vivo* Rubisco activity and mesophyll conductance accounted for 84% of the limitation whereas under non-steady-state conditions stomatal conductance was the major limitation contributing to 13% and 5% for losses in CO_2 uptake and water use efficiency, respectively. Triose phosphate utilization, while sufficient to support observed rates, would not allow improvements of CO_2 uptake of more than 33%.
- The variation of carbon assimilation among cultivars were three times greater under non-steady-state compared to steady-state, pinpointing important overlooked targets for improvement in photosynthesis in cassava.

Keywords: cassava breeding, food security, genetic engineering, *Manihot esculenta*, photosynthetic induction, Rubisco, Sub-Saharan Africa, yield potential.

INTRODUCTION

Rising global population coupled with increased urbanization is predicted to increase food demand by 60% until 2050. Demand increase will be greatest in Sub-Saharan Africa where population is expected to double by 2050 (van Ittersum *et al.*, 2016; United Nations, 2017). In this region, where cassava (*Manihot esculenta* Crantz) is the most planted crop (FAOSTAT, 2019a), food demand is projected to rise by 55% within just 15 years (World Bank, 2017). For a variety of cultural and pragmatic reasons, cassava is also the preferred staple food source for the small-holder farmers who constitute the bulk of the population. Dependence on cassava in Africa is underlined by the fact that it accounts for a higher proportion of food consumption per person than any staple in any part of the world (i.e., 0.4 kilograms per person/day) (Henry *et al.*, 2004). This makes cassava virtually irreplaceable in the fight against hunger in this key and most vulnerable region of the world (Nassar & Ortiz, 2010). Its importance as a cash crop has also increased with wider-spread usage by industry (Kleih *et al.*, 2013; Uchechykwu-Agua *et al.*, 2015). For small-farmers holders, increased yields mean that when family needs are exceeded, the surpluses can be sold to provide other household needs. However, cassava yield in Sub-Saharan Africa did not increase over the last 13 years (De Souza *et al.*, 2017; FAOSTAT, 2019b). Moreover, the genetic progress achieved in breeding programs for increased yield has slowed significantly in recent years (Ceballos *et al.*, 2016). In Africa, the focus has necessarily been on disease and pest resistance (Alene *et al.*, 2018). However, increasing yield also depends on increasing genetic yield potential, i.e. the yield that can be achieved in the absence of pests, disease, water and nutrient limitations.

Increased yield potential can be achieved by improving photosynthetic efficiency (Long *et al.*, 2006). Comparing the photosynthetic rates between landraces and improved lines, there is no evidence that photosynthesis in cassava has been improved through breeding (De Souza *et al.*, 2017; De Souza & Long, 2018). Indeed, the conversion efficiency in cassava, which reflects its

72 photosynthetic rates, is just one-seventh of the theoretical value for C_3 plants (De Souza *et al.*,
73 2017). The validation that increased photosynthetic efficiency can improve yield potential in
74 cassava has been shown by Free Air CO_2 Enrichment experiments (FACE). Under open-air field
75 CO_2 concentration elevation, leaf photosynthesis was increased by 30%, resulting in a doubling in
76 cassava yield (Rosenthal *et al.*, 2012). This shows that, if photosynthetic efficiency can be
77 genetically improved in cassava, yield potential will also be substantially increased.

78 Genetic improvements depend on the understanding of the pre-existing diversity for a
79 particular desired trait within an avaiable germplasm. For bioengineering strategies, it is also key
80 to understand the limitations of the desirable trait to design suitable approaches to overcome
81 identified limitations. In cassava, it is remarkable that the genetic variability in photosynthesis is
82 little known while limitations have not been analyzed (Ceballos *et al.*, 2004). Although the
83 diversity in steady-state photosynthesis of South American cassava cultivars has been evaluated
84 (El-Sharkawy, 2006; El-Sharkawy, 2016), very little is known about African germplasm (De
85 Souza *et al.*, 2017; De Souza & Long, 2018).

86 Under steady-state conditions, *in vivo* biochemical and diffusive limitations to leaf
87 photosynthesis may be deduced from the response of net leaf CO_2 uptake under saturating light
88 (A_{sat}) to intracellular CO_2 concentrations (c_i) (Long & Bernacchi, 2003). These limitations are the
89 apparent maximum *in vivo* Rubisco activity (V_{cmax}), maximum electron transport rate (J_{max}) and
90 the maximum rate of triose phosphate utilization (V_{TPU}). Mesophyll conductance to CO_2 diffusion
91 (g_m) is obtained by combining the A/c_i curves with modulated chlorophyll fluorescence (Harley *et*
92 *al.*, 1992). In a previous study, photosynthesis under steady-state in four African cassava cultivars
93 was found to be limited by V_{cmax}, which suggested that Rubisco activity and/or g_m were restricting
94 CO_2 uptake (De Souza & Long, 2018). While these results provided an indication that there was
95 genotypic variation, they did not account for the full range of quantitative limitations of

96 photosynthesis and indicated the need for evaluation of a larger number of farmer-preferred
97 cultivars to provide a more realistic assessment of the photosynthetic limitations under steady-state
98 conditions.

99 Improvement of photosynthetic efficiency has focused almost entirely on steady-state and
100 light-saturating conditions. However, in field crop canopies including that of cassava, lighting is
101 almost never at steady-state due to continuous fluctuations in light (Pearcy, 1990). While there is
102 limited information on steady-state photosynthesis and its limitations in cassava, there is none to
103 our knowledge on photosynthetic limitations under fluctuating light conditions. Critically, when a
104 leaf transitions from shade to full sunlight, there is a delay of minutes in achieving its maximum
105 photosynthetic rates. This delay can be caused either by the rate of activation of Rubisco (Mott
106 & Woodrow, 2000; Soleh *et al.*, 2016) or the rate of stomatal opening (Allen & Pearcy, 2000;
107 McAusland *et al.*, 2016). Depending on how slow this transition is, it adversely affects daily
108 photosynthetic carbon gain resulting in lower biomass production. In wheat, for instance, the slow
109 photosynthetic adjustment from shade to sun was calculated to result in a 21% loss of net canopy
110 CO_2 assimilation and productivity (Taylor & Long, 2017). Considering the converse situation,
111 when a leaf transitions from light to shade, photosynthesis declines immediately while stomatal
112 responses are much slower, lowering by ~ 20% the intrinsic efficiency of water use (Lawson &
113 Blatt, 2014). On such transitions, it also takes many minutes for photosynthesis to acclimate to the
114 lower light conditions, and over the course of a growing season this can cost 20 – 40% of potential
115 productivity (Zhu *et al.*, 2004; Kromdijk *et al.*, 2016). In cassava, there is no information on how
116 photosynthesis and stomatal conductance respond to fluctuations in light, nor what limits the speed
117 of adjustment and, in turn, efficiency. This information would be crucial for developing strategies
118 to improve carbon gain and water use efficiency in this species.

In addition to the physiological measurements, mechanistic models of photosynthetic metabolism provide a means to test hypothesis related to different *in vivo* dynamic behaviors, and provide a broader guide to assess quantitatively the value of varying traits affecting photosynthetic efficiency (Zhu *et al.*, 2007; Zhu *et al.*, 2013). Previous model predictions have determined potential routes for improvements in photosynthesis (Zhu *et al.*, 2004; Long *et al.*, 2006) that were later successfully translated to yield increases (Lefebvre *et al.*, 2005; Kromdijk *et al.*, 2016; South *et al.*, 2019). This approach is used here, integrating physiological and biochemical measurements to then predict modifications that could improve photosynthetic efficiency, and by how much.

Here we quantified limitations to photosynthesis in thirteen African farm-preferred and high yielding cassava cultivars under steady-state and fluctuating light conditions, aiming to determine the potential for improving cassava photosynthetic efficiency. A metabolic model of photosynthesis in cassava was developed using the measurements to explore the underlying traits that could give the largest improvements in photosynthetic and water-use efficiencies, with a focus on non-steady-state conditions.

METHODS

Plant material and growth conditions

Thirteen farm-preferred cassava (*Manihot esculenta* Crantz) cultivars from Africa were chosen for this study, including five landraces (MBundumali, TME3, TME419, TME7, and TME693) and eight improved lines (TMS01/1412, TMS30001, TMS30572, TMS96/1632, TMS97/2205, TMS98/0002, TMS98/0505, and TMS98/0581). Measurements were taken in two independent experiments (from May 23 to July 01 2017 and from May 01 to June 15 2018) in a controlled environmental greenhouse at the University of Illinois at Urbana-Champaign. This was except for cultivars TMS97/2205 and TMS98/0505 that were evaluated only in 2017. For both

experiments, all cultivars were propagated *in vitro* and transferred to the greenhouse as previously described in De Souza and Long (2018). Air temperature inside the greenhouse was 28°C ± 4°C, and relative air humidity was 61% ± 16%. In each experiment, three to four biological replicates of each cultivar were measured in a completely randomized experimental design. Pots were distributed with 25 cm spacing and their positions in the greenhouse re-randomized every 4-5 days to circumvent confounding cultivar with any environmental variation within the greenhouse. Plants were watered to pot capacity every 2-3 days allowing the soil surface to dry between the watering.

Gas exchange and assessment of photosynthetic limitations under steady-state

Leaf CO_2 assimilation of the central foliole of the youngest fully expanded leaf was measured on 40 days-old plants with a portable gas exchange systems integrated with a leaf cuvette including a modulated chlorophyll fluorometer and light source (LI-6400XT and LI-6400-40; LI-COR, Lincoln, NE, USA). For the response of leaf net CO_2 uptake to intracellular CO_2 concentration (A/c_i curves), the leaf was acclimated to a light intensity of 1500 µmol $m^{-2}s^{-1}$ (ca. 90% red and 10% blue light) and a CO_2 concentration of 400 µmol mol^{-1} inside the cuvette. After steady-states for both A and stomatal conductance (g_s) were obtained, the chamber inlet [CO_2] was varied according to the following sequence: 400, 270, 150, 100, 75, 50, 400, 400, 600, 800, 1100, 1300 and 1500 µmol mol^{-1}. The gas exchange measurements were recorded simultaneously with chlorophyll fluorescence as a 10s average after the conditions inside the cuvette were stable at each [CO_2]. The block temperature was set to 28°C, vapor pressure deficit (VPD) inside the cuvette was maintained at 1.5 ± 0.3 kPa and the flow at 300 µmol s^{-1}.

The apparent maxima of Rubisco carboxylation rate (V_{cmax}), regeneration of ribulose-1,5-biphosphate expressed as electron transport rate (J_{max}), and triose phosphate utilization (V_{TPU}) were

calculated from the A/c_i curves using the equations from von Caemmerer (2000). Before fitting the curves, values for each individual curve were corrected for diffusive leaks between the cuvette and external environment (Bernacchi *et al.*, 2001). Calculated values were adjusted to 25°C, following the equations for temperature response as described by Bernacchi *et al.* (2001) and McMurtrie and Wang (1993). Stomatal conductance and operating c_i were obtained from the data points collected at 400 µmol mol^{-1} of CO_2. The intrinsic water use efficiency (*iWUE*) was calculated by dividing A by g_s at this same CO_2 concentration.

Mesophyll conductance (g_m) and partial pressure of CO_2 inside the chloroplast (c_c) were calculated for ambient CO_2 concentration (ca. 400 µmol mol^{-1}) according to the variable J method (Harley *et al.*, 1992). The CO_2 compensation point (Γ^*) and respiration (R_d) values necessary for g_m calculation were estimated for each replicate according to Moualeu-Ngangue *et al.* (2017). V_{cmax} and J_{max}, based on chloroplast [CO_2] derived from measured g_m were obtained by using a nonlinear analysis with the Marquart method (Moualeu-Ngangue *et al.*, 2017).

To determine photosynthetic limitations under steady-state, the stomatal, mesophyll, and biochemical relative limitations were calculated following Grassi and Magnani (2005). Values for Rubisco Michaelis constants for CO_2 (K_c) and for O_2 (K_o) in these calculations were from Bernacchi *et al.* (2001).

Gas exchange and quantification of diffusional and biochemical limitations under fluctuating light conditions

To evaluate the response of gas exchange in cassava under fluctuating light, two measurements were performed: (a) photosynthetic response to the transition from deep shade to high light (i.e. induction curves), and (b) photosynthetic response to the transition from high to low to high light (i.e. relaxation curves followed by induction curves). The measurements were

191 performed on 35-40 days-old plants using the same equipment described above for the steady-state
192 measurements.

193 For the induction curves, plants were maintained in the dark overnight. Before the
194 measurements, the central foliole of the youngest fully expanded leaf was acclimated to the
195 conditions of the LI-6400 cuvette for 20 min, still in the dark. CO_2 concentration inside the cuvette
196 was 400 µmol mol^{-1}, air temperature 28°C ± 2°C, and VPD 1.5 ± 0.3 kPa. After 20 min, leaves
197 were pre-illuminated with 50 µmol $m^{-2}s^{-1}$ (deep shade) of photosynthetic photon flux density
198 (PPFD) for 5 min to induce photosynthesis. Then, the light was increased to PPFD of 1500 µmol
199 $m^{-2}s^{-1}$ for 30 min, simulating a shade-sun transition. Gas exchange parameters were recorded every
200 10s. For each induction curve, the time to reach 50% of maximum photosynthesis (T_{50A}), the time
201 to reach 90% of maximum photosynthesis (T_{90A}), the cumulative CO_2 fixation in the first 5 min
202 after photosynthetic induction (CCF), and the time to reach 50% of maximum stomatal
203 conductance (T_{50gs}) were calculated. The maximum light-saturated leaf CO_2 uptake and maximum
204 stomatal conductance in the induction curves were considered to be that obtained after 30 min
205 under high light. The stomatal conductance at the beginning of induction (g_{sT0}) was the last value
206 obtained before increasing the light to 1500 µmol $m^{-2}s^{-1}$ PPFD. To investigate the impact of the
207 rate at which the stomata opened on the induction of photosynthesis, a similar induction curve was
208 performed, using a low CO_2 concentration of 100 ppm inside the chamber during the deep shade
209 period to maintain stomatal opening (Taylor & Long, 2017).

210 The variation in induction rates of three cultivars with contrasting responses were further
211 evaluated with induction curves at five CO_2 concentrations (75, 150, 270, 400 and 600 µmol mol^{-1}
212 of CO_2). From these curves, V_{cmax} and stomatal limitation under non-steady-state conditions were
213 calculated using the equations described by Soleh *et al.* (2016).

Acclimation of photosynthesis to shade, on a sun-shade transition, was characterized after a steady-state rate of leaf CO_2 uptake was obtained at 1500 µmol $m^{-2}s^{-1}$ PPFD (~ 40 minutes). Once in steady-state, the light was decreased to 10% of the initial value (i.e., 150 µmol $m^{-2}s^{-1}$ PPFD), and plants were kept under this light intensity for 40 minutes. Then, the light was increased to 1500 µmol $m^{-2}s^{-1}$ PPFD again, for an additional 40 minutes. Gas exchange was recorded every 10s. Rate constants were calculated for the increase in g_s on transfer to 1500 µmol $m^{-2}s^{-1}$ PPFD (k_i), and again for the decrease in g_s on return to 150 µmol $m^{-2}s^{-1}$ PPFD (k_d). Measured time series for stomatal conductance changes were fit to the following equation:

$$g_s = (g_{max} - g_0)e^{-kt} + g_0$$

where: g_{max} is the maximum stomata conductance, g_0 is the minimum stomata conductance, t is time, and k (k_i or k_d) is the value calculated by the curve fitting function (fit) in MATLAB (The Mathworks, Inc®).

Rubisco and Rubisco activase contents, Rubisco activity, total soluble protein and chlorophyll assays

Leaf samples of 4 cm^2 were collected, snap frozen and stored at -80°C until analysis. Samples were homogenized using an ice-cold mortar and pestle in 0.6 mL of extraction buffer (50 mM Bicine-NaOH pH 8.2, 20 mM $MgCl_2$, 1 mM EDTA, 2 mM benzamidine, 5 mM ε-aminocaproic acid, 50 mM 2-mercaptoethanol, 10 mM dithiothreitol, 1% (v/v) protease inhibitor cocktail (Sigma-Aldrich, Mo, USA), and 1 mM phenylmethylsulphonyl fluoride). After rapid (45 – 60 s) grinding, samples were clarified via centrifugation at 4°C, 14700×*g* for 1 min. The supernatant was used immediately to determine the initial and total activity of Rubisco via incorporation of $^{14}CO_2$ into acid-stable products at 25°C (Parry *et al.*, 1997; Carmo-Silva *et al.*, 2017). This involved a reaction mixture containing 100 mM Bicine-NaOH pH 8.2, 20 mM $MgCl_2$,

10 mM $NaH^{14}CO_2$ (9.25 kBq µmol^{-1}), 2 mM KH_2PO_4, and 0.6 mM RuBP. Assays of initial activity were started by the addition of 25 µL supernatant to the complete assay mixture, whilst total activity assays were started by addition of RuBP to the mixture 3 min after adding 25 µL of the supernatant, to allow full carbamylation of Rubisco in the presence of CO_2 and Mg^{+2} prior to the assay. All reactions were quenched after 30s by adding 100 µL of 10 M formic acid. Assay mixtures were dried at 90°C and 0.4 mL de-ionized water added to re-dissolve the residue. Acid-stable ^{14}C was determined by scintillation counting (Packard Tri-Carb, PerkinElmer, UK) with the addition of 3.6 mL of scintillation cocktail (Gold Star Quanta, Meridian Biotechnologies, UK). The incubation time for total activity was tested to ensure accurate determination of total activity (Sharwood *et al.*, 2016), and three minutes was found to be sufficient. Rubisco activation state was calculated as the ratio of initial to total activity. 100 µL of the same supernatant was incubated at RT for 30 min with 100 µL of buffer containing 100 mM Bicine-NaOH pH 8.2, 20 mM $MgCl_2$, 20 mM $NaHCO_3$, 1.2 mM (37 kBq/µmol) [^{14}C]CABP (carboxyarabinitol-1,5-bisphosphate), and Rubisco content determined via [^{14}C]CABP binding (Sharwood *et al.*, 2016).

Total soluble protein (TSP) was determined via Bradford assay (Bradford, 1976). Chlorophyll determination followed the method described by Wintermans and de Mots (1965). 20 µL of the homogenate was rapidly taken in duplicate prior to centrifugation and added to 480 µL ethanol, inverted to mix, and kept in the dark until all extractions were complete (Carmo-Silva *et al.*, 2017). Chlorophyll content was determined by measuring absorbance using a microplate reader (SPECTROstar Nano, BMG LabTech, UK).

To determine relative Rubisco activase content, an aliquot of the supernatant resulting from Rubisco analysis was mixed 1:1 with SDS-Page loading buffer (62.5 mM Tris-HCl, pH 6.8, 2% (w/v) SDS, 25% (v/v) glycerol, 0.01% bromophenol blue), mixed by pipetting and heated at 95°C for 4 min. Proteins were separated via SDS-Page (12% TGX gels, Bio-Rad, UK), and transferred

to a nitrocellulose membrane using a dry blotting system (iBlot2, ThermoFisher Scientific, UK) (Perdomo *et al.*, 2018). Rubisco activase was detected using an antibody with broad specificity for both isoforms of the protein in higher plants (Feller *et al.*, 1998), and a secondary fluoro-tagged antibody (IRDye800CW, LI-COR Biosciences, Lincoln NE, USA). Images were taken and protein amounts quantified using a fluorescence imaging and analysis system (Odyssey FC, LI-COR Biosciences, Lincoln NE, USA). Due to uncertainty regarding the exact binding affinity of this antibody to cassava Rubisco activase, after densitometry of all samples, signal intensities were compared relative to the mean signal intensity of the entire dataset to provide relative quantification of the panel of cultivars.

Cassava photosynthesis model and photosynthetic simulations

To estimate the influence of stomata and Rubisco response on dynamic photosynthesis rate, a cassava photosynthesis metabolic model was developed. The model was constructed based on the C_3 photosynthesis model (Zhu *et al.*, 2007), a simplified light reaction model, a Rubisco activase model (Mate *et al.*, 1996; Zhu *et al.*, 2013), and a dynamic stomatal conductance model (Vialet-Chabrand *et al.*, 2017). The model was implemented in MATLAB. The full description of the model is in Supplemental Notes S1.

The model was parameterized using V_{cmax}, J_{max}, k_i, k_d, Ball-Berry slope and intercept from measured photosynthetic and stomata parameters of cassava (Supplemental Table S4). The measured V_{cmax} was used as the maximum Rubisco activity in the metabolic model. A, transpiration (T), c_i, and g_s were estimated under a fluctuating light cycle. The predicted water use efficiency (WUE) was calculated dividing A by T.

286 **Statistical analysis**

287 Differences between cultivars were tested by analysis of variance (ANOVA) or non-
288 parametric methods (JMP®Pro, version 12.0.1; SAS Institute INC, Cary, NC, USA). For all
289 measured variables, the normality was tested using the Shapiro-Wilk's test and the
290 homoscedasticity using Brown-Forsythe's and Levene's tests. When the data met the criteria for
291 normality and homoscedasticity assumptions, one-way ANOVA followed by a pairwise
292 comparison (*t*-test) was applied. When those criteria were violated, Wilcoxon's non-parametric
293 comparison was used. The threshold for statistical significance was $P \leq 0.05$. The data were
294 analyzed using a completely randomized block design, split over two years. The extent of
295 correlation between steady-state variables were evaluated using Pearson's correlation using the
296 data of all cultivars.

297

298 **RESULTS**

299 **Cassava photosynthetic limitations under steady-state**

300 Light-saturated net leaf CO_2 uptake (A_{sat}) in cassava cultivars ranged from 20.3 to 24.8
301 µmol $m^{-2}s^{-1}$, a total variation of 20% between cultivars (Table 1). A similar 20-24% range of
302 variation was also observed for V_{cmax} and J_{max} calculated from the response of A_{sat} to c_i, and V_{cmax}
303 calculated from c_c ($V_{cmax,Cc}$) (Table 1). Because estimation of c_c cannot be calculated by the
304 variable *J* method when there is triose phosphate limitation due to the decrease in electron transport
305 rate (Harley *et al.*, 1992), values of $J_{max,Cc}$ could not be calculated for cassava plants in this
306 experiment. However, under high c_i the effect of g_m on A_{sat} is small (Harley *et al.*, 1992). The
307 operating c_i for all cultivars were below the transition in the A/c_i response from Rubisco limitation
308 to electron transport limitation (Fig.1), indicating that all cassava cultivars are Rubisco limited at
309 current atmospheric [CO_2]. Stomatal conductance (g_s) varied from 0.25 to 0.34 mol H_2O $m^{-2}s^{-1}$

leading to a 26.5% of variation in intrinsic water use efficiency (*iWUE*) among cultivars (Table 1). TMS97/2205 cultivar showed the highest *iWUE* whereas TMS96/1632 and TMS01/1412 had the lowest *iWUE* values out of the cultivars surveyed (Table 1).

Corroborating the data presented above, the calculation of relative photosynthetic limitation by the method of Grassi and Magnani (2005) showed that, despite no significant differences among cultivars (Supplemental Fig.S1), at current atmospheric [CO_2] *in vivo* Rubisco activity accounted for about 43% of the total limitation across all cultivars, while stomatal conductance accounted for 16% (Fig.2). Mesophyll conductance (g_m) did not vary significantly among cultivars (Supplemental Fig.S2). However, it did account for a similar proportion (i.e. 41%) of the total limitation to photosynthesis across cultivars in cassava (Fig.2). Additionally, g_m wa positively correlated to A_{sat} (r=0.27, P=0.042; Supplemental Table S2).

For most cultivars, A did not increase significantly when measured at c_i higher than 700 µmol $m^{-2}s^{-1}$ (Fig.1). Except for TMS98/0505 and TMS97/2205 that increased photosynthesis by 7.7% and 5.1%, respectively, from c_i of ~800 µmol $m^{-2}s^{-1}$ to c_i of ~1250 µmol $m^{-2}s^{-1}$, all other cultivars showed, on average, only 2.6% increase in photosynthesis under c_i higher than 700 µmol $m^{-2}s^{-1}$. The lack of increase in photosynthesis with an increase in c_i suggests that a TPU limitation is present in the majority of cassava cultivars evaluated in this study. This is further supported by the observed concomitant reduction in J_{PSII} (6 – 16%) with increasing c_i (Fig.1). There was a significant 15% variation in V_{TPU}, which ranged from 9.9 to 11.65 µmol $m^{-2}s^{-1}$ (Table 1). On average, V_{TPU} for cassava was 10.8 µmol $m^{-2}s^{-1}$, suggesting a TPU utilization 44% above the average A_{sat}.

Rubisco content, Rubisco initial, total and specific activity, and Rubisco activation state varied significantly among cultivars (Supplemental Table S1). The variation of Rubisco content, and initial and total activity was positively correlated to A_{sat} (r=0.46, P=0.001; r=0.36, P=0.012;

and r=0.36, P=0.011, respectively; Supplemental Table S2). Rubisco content also correlated with V_{cmax} (r=0.37, P=0.009). Total Rubisco activase and fractions of α and β Rubisco activase isoforms did not vary significantly (Supplemental Table S1). Chlorophyll *a* (Chl*a*), *b* (Chl*b*), total and the ratio of Chl*a*/Chl*b* showed significant differences among cultivars (Supplemental Table S3). From these, Chl*a*/Chl*b* ratio presented a significant correlation with A_{sat} (r=0.30, P=0.029; Supplemental Table S2). Variation in total soluble protein content (TSP) and in the ratio of TSP to chlorophyll (TSP/Chl) content between cultivars (Supplemental Table S3) did not correlate with variation in A_{sat} (Supplemental Table S2).

Dynamic photosynthesis and its limitations in cassava

Induction of photosynthesis on transfer from deep shade (50 µmol $m^{-2}s^{-1}$ PPFD) to high light (1500 µmol $m^{-2}s^{-1}$ PPFD) was at significantly different rates across the cassava cultivars (P<0.0001; Fig.3a). TMS98/0505 showed the fastest induction, reaching 50% and 90% of the steady-state A_{sat} after 3 and 11 minutes, respectively. TME693 had the slowest induction rates with more than 10 and 21 minutes to reach, respectively, 50% and 90% of steady-state A_{sat} (Fig.3a, Table 2). These differences in photosynthetic induction rates translated to a variation of 65% in the cumulative carbon fixation (CCF) (Table 2), which correspond closely to stomatal opening, as represented by g_s (Fig.3b, Table 2). Both stomatal conductance at the beginning of the induction (g_{sT0}) and time to reach 50% of the final steady-state g_s (T_{50gs}) had a significant correlation with CCF (r=-0.60, P<0.0001 and r =0.52, P<0.0001). Despite the differences in induction rates, after 30 minutes the photosynthetic rates of all cultivars reached similar values to those obtained at steady-state (Supplemental Fig.S3, Table 1). During photosynthesis induction, *iWUE* also varied among cultivars (Fig.3d). During the first 5 minutes of induction, *iWUE* in TME7 was 2-fold higher than in TMS 98/0505.

The role of g_s on the speed of photosynthetic induction was investigated on the three selected cultivars by keeping the stomata open in low light, by reducing the chamber [CO_2] around to 100 µmol mol^{-1} during the low light phase. Here, induction in high light was far more rapid and did not differ between cultivars (Fig.4c). Differences in the speed of induction were therefore due to differences in the speed of stomatal opening.

Biochemical and stomatal limitations during induction in cassava were further estimated by measuring photosynthetic induction in different CO_2 concentrations. With these data, A/c_i curves were fit for different time points during the inductions (Supplemental Fig.S4), and V_{cmax} and stomatal limitation were calculated (Fig.5). The initial phase of the A/c_i curves increased with induction for the three cultivars, and no significant differences were observed (Supplemental Fig.S4). This was reflected in a non-significant difference in V_{cmax} calculated for this phase across these cultivars (Fig.5a), suggesting that Rubisco activity is not responsible for the differences observed during the induction. Nevertheless, the operating c_i in all three cultivars is in the Rubisco-limited part of the A/c_i curve throughout the induction (Supplemental Fig.S4), indicating that the induction response in cassava cultivars is overall Rubisco limited. Stomatal limitation during induction is higher in TME693 than in TMS98/0505 (Fig.5b), especially during the first 5 minutes (Fig.5c) where there is a 20% difference (P=0.034) between the two cultivars. Corroborating this, the c_i during the first 5 minutes of induction under ambient [CO_2] is 15.5% lower than the c_i under steady-state (Fig.3c). The stomatal limitation in TME693 decreases after approximately 15 minutes of induction and, after this period, it is similar to the stomatal limitation of the other two cultivars (Fig.5b).

On transfer from high-light to shade, A decreases instantaneously but g_s required more than 20 minutes to reach steady-state in all cassava cultivars (Supplemental Fig.S5). Consistent with the differences in induction described above, TME693 showed low values of both rate constant

for g_s increase (k_i) and for g_s decrease (k_d) (Supplemental Table S4), indicating that slow opening corresponded to slow closing. By contrast, TMS01/1412, that has similar rates of photosynthesis induction to TMS98/0505 (Table 2, Supplemental Fig.S3), showed the highest k_i and a high k_d (Supplemental Fig.S4). However, correspondence of k_d with k_i was not apparent across all cultivars.

Model simulations

Values of V_{cmax}, J_{max}, k_i, k_d and Ball-Berry parameters (Supplemental Table S4) were used to simulate carbon assimilation and stomatal response in two contrasting cultivars, TME693 and TMS01/1412 (Fig.6). These simulations were done considering the dynamic changes in Rubisco activation (DyRac) and dynamic stomatal conductance response (DyGs). The incorporation of these two variables improved the model performance adjudged by an improved match to the measured induction curves (Supplemental Fig.S6). The model showed that accelerating stomatal response three times would increase average *A* 11% for TME693 and 7% for TMS01/1412, during the first 10 min of induction (Fig.6, Supplemental Table S5). After 10 min of induction, and during low and high light phases, there is no significant impact (i.e., <3%) of acceleration of stomatal response on *A*. However, acceleration in stomatal response decreases ~15% *WUE* in TME693 over the first 30 min of photosynthesis induction. For TMS01/1412, this reduction is ~ 12% during the first 20 min of induction. There is also a decrease in *WUE* by 8% during the first 20 min of high light for both cultivars. However, *WUE* increases by 20% in TME693 and by 13% in TMS01/1412 during the first 20-30 min of low light, by accelerating the speed of decline in g_s (Fig.6, Supplemental Table S5).

The model was also used to simulate *A* and *WUE* in a cycle of low and high light, simulating the fluctuation of light that occurs in lower layers of the canopy. This was applied to

406 all cultivars with and without the incorporation of dynamic stomata response in the simulations
407 (Supplemental Fig.S7). The results showed that with the light fluctuation, there was an average of
408 13% loss of carbon assimilation and 5% of *WUE* resulted from the lags in stomatal response.
409 Accelerating stomata opening and closure speed in three times, can offset 6% this carbon loss, and
410 2% of *WUE* (Supplemental Fig.S7b).
411
412 **DISCUSSION**
413 Overcoming photosynthetic limitations to improve photosynthetic efficiency at the leaf-
414 level has resulted in some large demonstrated increases in field crop productivity and water use
415 efficiency (Kromdijk *et al.*, 2016; Glowacka *et al.*, 2018; Simkin *et al.*, 2019; South *et al.*, 2019).
416 The past focus has been overwhelmingly on light-saturated steady-state photosynthesis. However,
417 in field crop canopies, half of carbon gain is under conditions where photosynthesis is light-limited
418 and most leaves are rarely in steady-state light (Zhu *et al.*, 2004; Taylor & Long, 2017; Papanatsiou
419 *et al.*, 2019). While steady-state measurements are valuable for quantification of biochemical
420 limitations *in vivo* (Long & Bernacchi, 2003), dynamic measurements provide insight into the
421 more frequent field condition, particularly in crops canopies, of how leaves respond to fluctuating
422 light (Way & Pearcy, 2012). Indeed, variation between cassava cultivars in carbon assimilation
423 under non steady-state conditions was three times that of steady-state (Tables 1 and 2), identifying
424 important new traits for selection in improving cassava photosynthetic efficiency and yield
425 potential.
426
427 **Biochemical and mesophyll limitations play a major role in photosynthesis under steady-**
428 **state**

Similar to other C_3 crops (Xiong *et al.*, 2018), biochemical limitation at steady-state was 43% of the total photosynthetic limitation in cassava (Fig.2). *In vivo* Rubisco activity, not regeneration of RuBP, accounted for this biochemical limitation under the current atmospheric CO_2 concentration, since operating c_i for all cultivars was below the transition from Rubisco to electron transport limitation (Fig.1). On average, Rubisco content in cassava was 1.6 g m^{-2} (Table S1). This is lower to 3 g m^{-2} for wheat and 2.6 g m^{-2} for rice, under similar conditions of good nutrition (Theobald *et al.*, 1998; Masumoto *et al.*, 2005). Although the CO_2 specificity of Rubisco in cassava is slightly higher ($S_{c/o}$ at 25°C= 105.4 ± 1.8) than in both rice and wheat ($S_{c/o}$ at 25°C= 101 ± 2 and 100 ± 1.1, respectively), its carboxylation efficiency of Rubisco (k_{cat}^{c}/k_{c}^{air}) is approximately 30% lower (Orr *et al.*, 2016). Lower content and efficiency would explain the lower V_{cmax} in cassava (Table 1) compared to elite cultivars of soybean, wheat and rice (Masumoto *et al.*, 2005; Driever *et al.*, 2014; Koester *et al.*, 2014). This difference between cassava and these other C_3 crops suggest that strategies proposed to improve Rubisco efficiency and quantity would have particular value with this crop (Parry *et al.*, 2007; Whitney *et al.*, 2011; Carmo-Silva *et al.*, 2015). The 20% between cultivar variation in V_{cmax} found here, while less than the 35% and 55% observed in rice and soybean, respectively (Gu *et al.*, 2012; Koester *et al.*, 2014), would still provide a basis for breeding a significant improvement in photosynthetic efficiency.

The limitation to steady-state photosynthesis imposed by mesophyll conductance approached that imposed by assimilation within the chloroplast (ca. 41%, Fig.2). This is more than double the limitation imposed by stomata (Fig.2). Increasing g_m is an attractive target for breeding or bioengineering, since it can increase photosynthesis without increasing transpiration (Flexas *et al.*, 2008; Zhu *et al.*, 2010). An extensive survey of South American cultivars showed that differences in photosynthesis, biomass and yield were closely associated with variation in g_m (El-Sharkawy & Cock, 1990; El-Sharkawy *et al.*, 1990; El-Sharkawy *et al.*, 2008). This is consistent

453 with the correlation between g_m and A_{sat} found here for African cultivars (Table S2). However,
454 there is no evidence that g_m has been increased with breeding, with no significant difference
455 between g_m in landraces and improved lines (F = 0.02; P=0.889) suggesting that efforts to increase
456 g_m in cassava might lead to a significant improvement in photosynthetic rate in this crop.

457 Simulations have shown that increasing either V_{cmax} or g_m could compensate for up to a
458 40% decrease in stomatal conductance to water vapor (g_{sw}) (Flexas *et al.*, 2016). This would allow
459 a cultivar to maintain the same A_{sat} while using 40% less water, i.e. a 40% increase in *iWUE*.
460 Although manipulations in g_m have been found to affect g_s negatively in some other species (Hanba
461 *et al.*, 2004; Flexas *et al.*, 2006), these two parameters were not significantly correlated in cassava
462 (r=0.14, P= 0.280; Table S2). A similar lack of correlation was also found across cultivars of
463 wheat, supporting the contention that improved g_m may be selected without impacting g_s (Jahan *et*
464 *al.*, 2014; Barbour *et al.*, 2016). In cassava this would not only increase in A_{sat} under optimal
465 conditions, but increase its resilience to the frequent and increasing droughts affecting the major
466 growing regions of Sub-Saharan Africa (Tadele, 2018).

467

468 **Low capacity of triose phosphate utilization (TPU) may limit photosynthetic improvements**

469 While Rubisco and mesophyll conductance are the major limitations found in cassava
470 under the current rates of photosynthesis, TPU limitation, which reflects the plant's ability to
471 convert triose phosphates into sucrose and starch (Sharkey, 1985), can represent a major hurdle
472 for improving photosynthesis in this crop. Eleven of the thirteen cassava cultivars evaluated
473 showed TPU limitation, at an A_{sat} only slightly higher than the A_{sat} measured at the current ambient
474 [CO_2]. This was evident as a lack of any increase in A_{sat} when c_i exceeded 700 µmol $m^{-2}s^{-1}$ and a
475 decline in J_{PSII} (Fig.1)(Sharkey, 1985; Long & Bernacchi, 2003). The average V_{TPU} across the
476 cassava cultivars was 10.8 µmol $m^{-2}s^{-1}$ and only sufficient to support a maximum A_{sat} of 32 µmol

477 $m^{-2}s^{-1}$. Therefore, that maximum improvement in photosynthesis that could be bred or
478 bioengineered could not exceed 33% without simultaneous improvement of V_{TPU}. V_{TPU} here were
479 similar to those found in a more limited subset of African cassava cultivars (De Souza & Long,
480 2018), and 25.5% to 42% lower than in rice, wheat and rye (Wullschleger, 1993; Jaikumar *et al.*,
481 2013). Low rates of V_{TPU} can be associated with reduced sink strength for growth or storage, or
482 with insufficient capacity to synthesize sucrose and starch in the leaf (Long & Bernacchi, 2003;
483 Sharkey *et al.*, 2007). Cassava produces large tuberous roots. Thus, it is not expected that a reduced
484 sink strength would cause its low V_{TPU}. However, tuberous roots start to develop only after 2-3
485 months of planting (De Souza *et al.*, 2017), and our measurements were performed prior to that,
486 which would indicate a limitation during the plant's establishment phase (De Souza & Long,
487 2018). Nevertheless, failure to utilize fully photosynthetic potential, even before storage roots form
488 will be at the cost of canopy and root expansion during the critical establishment phase of the crop.
489 Suggested strategies that involve upregulation of AGPase in roots, and ADPglucose
490 pyrophosporylase and pyrophosphatase in leaves to enhance sucrose and starch synthesis (Ihemere
491 *et al.*, 2006; Jonik *et al.*, 2012; Yang *et al.*, 2016; Sonnewald & Fernie, 2018) may increase V_{TPU}
492 in cassava, and allow greater bioengineered or bred increases in photosynthesis.
493
494 **Slow stomatal conductance limits carbon fixation during light fluctuations**
495 After the transition from deep shade or low light to high light, cassava takes approximately
496 20 minutes to reach photosynthetic rates comparable to steady-state (Fig.3a, Fig.S3, Fig.S5).
497 Cumulative carbon fixation (CCF) over first five minutes varied 286%, from 122 for TME693 to
498 349 μmol CO_2 for TMS98/0505 (Table 2). What limits CCF in cassava? In tobacco, rice, soybean
499 and wheat, Rubisco activation is the major limitation to induction (Hammond *et al.*, 1998; Yamori
500 *et al.*, 2012; Soleh *et al.*, 2016; Taylor & Long, 2017), but in cassava, it is the rate of stomatal

opening (Fig.3). While the V_{cmax} during the induction was similar between the contrasting cultivars, stomatal limitation in the first 5 minutes varied substantially (Fig.5). When stomata limitation was removed by artificially lowering the chamber [CO_2] during shade, differences between cultivars in the speed of induction were eliminated (Fig.4).

The rate constant for g_s increase (k_i) varied 47% between cultivars with an average value of 9.8 minutes (Table S4). By definition, the higher the k_i the slower is the rise in g_s. The measured k_i for cassava were similar to those reported for tomato, wheat and common beans, but were eleven times higher than in rice, and three times higher than in maize (McAusland *et al.*, 2016). Slow stomatal opening during induction can significantly affect the CO_2 uptake and have a cumulative effect over the growing season, lowering yields (Reynolds *et al.*, 1994; Fisher *et al.*, 1998; Lawson & Blatt, 2014). Therefore, cultivars with an increased k_i, or any genetic manipulation that would allow acceleration of opening would benefit photosynthesis in cassava. Our simulations showed that with a three times acceleration of k_i, it is possible to increase photosynthetic carbon gain by 7%-11% during the first 10 minutes after induction from deep shade (Table S5). The large, almost 3-fold, differences found between cultivars during induction (Table 2) could, therefore, be exploited to improve cassava yield. Compared to the just 20% variation in steady-state photosynthesis (Table 1), this emphasizes non steady-state photosynthesis as an overlooked trait for improving cassava productivity.

Accelerating stomatal opening can cause a pronounced decrease in *WUE*. This is because the rate of transpiration through the stomata is higher than the rate of CO_2 assimilation due to the intrinsic differences in water and CO_2 concentration gradients between the intracellular spaces and the external atmosphere (Lawson & Blatt, 2014). To counterbalance the decrease of *WUE* when k_i is accelerated (Fig.6; Table S5), it is also necessary accelerate the rate of stomatal closing. Thus, when photosynthesis decreases due to a reduction in PPFD, stomata can close faster limiting the

water losses by transpiration, and therefore improving *WUE*. For the majority of cassava cultivars, the rate constant for g_s decrease (k_d) were lower than its k_i (Table S4), indicating that cassava stomata are faster to close than open. Yet, the average value of k_d in cassava is higher than for many other crops such as rice, maize, common beans, oat, tomato, sorghum, and wheat (McAusland *et al.*, 2016). Our modeling showed that a three-fold increase in k_i and k_d would increase *WUE* by 16%-20% during the transition from high to low light depending on the genotype (Fig.6; Table S5). Considering a cycle of fluctuations in light similar to that observed in lower layers of the canopy, this increase in k_i and k_d would increase daily carbon assimilation 6% without significant changes in water use efficiency (Fig.S7). Importantly, 6% would be the minimum gain in productivity, since prior to canopy closure this would have a positive feedback by creating more leaf and, in turn, more canopy carbon gain. Thus, over the cassava full growth cycle of 10 to 12 months (Lebot, 2009), a substantially higher gain in carbon would be expected while maintaining the current *WUE*.

ACKNOWLEDGMENTS

Technical support provided by Jerry Parng (University of Illinois) and by Dr. Rhiannon Page (Lancaster) is gratefully acknowledged. Authors also thank David Drag and Ben Harbaugh (University of Illinois) for greenhouse maintenance. The Rubisco activase antibody was a gift from Dr. Mike Salvucci (USDA-ARS). This work is supported by the research project Realizing Increased Photosynthetic Efficiency (RIPE) that is funded by the Bill & Melinda Gates Foundation, Foundation for Food and Agriculture Research (FFAR), and the UK Department for International Development (UKAid) under grant number OPP1172157.

549

550

551 **SUPPORTING INFORMATION**

552

553 **Fig. S1** Relative biochemical, mesophyll and stomatal limitations under steady state in cassava
554 cultivars

555 **Fig. S2** Mesophyll conductance in cassava cultivars

556 **Fig. S3** Changes in carbon assimilation during photosynthesis induction

557 **Fig. S4** Dynamic *A/ci* curves

558 **Fig. S5** Changes in leaf carbon assimilation, stomatal conductance, and intrinsic water efficiency
559 during light fluctuation

560 **Fig. S6** Simulated carbon assimilation rate, transpiration rate, intercellular CO_2 concentration, and
561 stomata conductance

562 **Fig. S7** Light input used in the model simulations and its results

563 **Table S1** Rubisco content, initial and total activity, Rubisco activation state, Rubisco specific
564 activity, total Rubisco activase, fraction of α and β isoforms of Rubisco activase

565 **Table S2** Matrix with values obtained from Pearson's correlation and its p-values

566 **Table S3** Chlorophyll contents, total soluble protein content, fraction of total soluble protein
567 present as Rubisco, and ratio of total soluble protein to chlorophyll content

568 **Table S4** Input parameters of cassava model

569 **Table S5** The effect of accelerating three times the stomata response speed on carbon assimilation
570 rate and water use efficiency

571 **Notes S1** Cassava model description

572

573

574

575 **LEGENDS TO FIGURES AND TABLES**

576

577 **Figure 1.** Response of light-saturated leaf carbon assimilation (*A,* µmol CO_2 $m^{-2}s^{-1}$) and of electron
578 transport rate (J_{PSII}) to intracellular CO_2 concentration (c_i) in cassava cultivars. Symbols represent
579 mean ± SE. n = 8, except for TMS98/0505 and TMS97/2205 where n=4. Larger symbols indicate
580 the operating point, which is at c_i achieved when the [CO_2] concentration around the leaf is 400
581 µmol mol^{-1}

582

583 **Figure 2**. Relative biochemical, mesophyll and stomatal limitations under steady state in cassava.
584 The total limitation is equal to 100%. Bars represent mean ± SE of all cultivars. Different letters
585 represent statistically significant differences (P<0.05) between different limitations.

586

587 **Figure 3.** Changes in leaf carbon assimilation (A, µmol CO_2 $m^{-2}s^{-1}$) **(a)**, stomatal conductance (g_s,
588 mol H_2O $m^{-2}s^{-1}$) **(b)**, internal CO_2 concentration (c_i, µmol CO_2 $m^{-2}s^{-1}$) **(c)**, and intrinsic water use
589 efficiency (*i*WUE, µmol CO_2 mol H_2O^{-1}) **(d)** in cassava cultivars during photosynthesis induction.
590 Relative values were calculated as the percentage of the value obtained after 30 minutes under
591 high light. During low light and high light phase, the light was 50 µmol $m^{-2}s^{-1}$ and 1500 µmol $m^{-2}s^{-1}$ PPFD, respectively. Colored lines indicate cultivars with contrasting responses (TME693 and
593 TMS98/0505) and the cultivar TME7. Data represent mean. n = 6 except for genotypes
594 TMS98/0505 and TMS97/2205 where n = 3.

595

596 **Figure 4.** Leaf carbon assimilation (A, μmol CO_2 $m^{-2}s^{-1}$) during induction with CO_2 concentration
597 during low light phase set at 400 ppm **(a)** or 100 ppm **(b)**. During the high light phase of the
598 induction, CO_2 concentration was maintained at 400 ppm in both measurements. Comparison
599 among cultivars related to time to reach 50% of light-saturated leaf carbon assimilation (T_{50A}, min),
600 time to reach 90% of light-saturated leaf carbon assimilation (T_{90A}, min), cumulative CO_2
601 concentration in the first 5 min after photosynthesis induction (CCF), and stomatal conductance at
602 the beginning of photosynthesis induction (g_{sT0}, mol H_2O $m^{-2}s^{-1}$) in both CO_2 concentrations during
603 low light phase **(c)**. Values represent mean ± SE. n=6 for TME693 and TME7; n=3 for
604 TMS98/0505. Different letters represent statistically significant differences (P<0.05) among the
605 cultivars.
606
607 **Figure 5.** Maximum carboxylation rate by Rubisco (V_{cmax}, μmol $m^{-2}s^{-1}$) **(a)** and stomatal limitation
608 during photosynthesis induction **(b,c)** in three cassava cultivars. Data represent mean ± SE. n=3-
609 4.
610
611 **Figure 6.** Model simulated carbon assimilation rate (A), transpiration rate (T), intercellular CO_2
612 concentration (c_i) and stomata conductance (g_s) of cultivars TME693 and TMS01/1412. Light in
613 PPFD input is: 0 μmol m^{-2} s^{-1} in the first 30 min, 50 μmol m^{-2} s^{-1} from 30 min to 35 min, 1500μmol
614 m^{-2} s^{-1} from 35 min to 75 min; 150μmol m^{-2} s^{-1} from 75 min to 115 min; and 1500 μmol m^{-2} s^{-1}
615 from 115 min to 155 min. Name of the cultivars followed by k_i*3 or k_i*3 k_d*3 represents the
616 simulation considering the acceleration by three time of the stomata opening and stomata opening
617 and closure, respectively.
618

Table 1. Light-saturated leaf carbon assimilation (A_{sat}, µmol CO_2 $m^{-2}s^{-1}$), apparent maximum carboxylation rate by Rubisco (V_{cmax}, µmol $m^{-2}s^{-1}$), maximum carboxylation rate by Rubisco estimated based on partial pressure of CO_2 inside the chloroplast ($V_{cmax,\ Cc}$, µmol $m^{-2}s^{-1}$), regeneration of ribulose-1,5-bisphosphate represented by electron transport rate (J_{max}, µmol $m^{-2}s^{-1}$), triose phosphate utilization ($V_{TPU,}$ µmol $m^{-2}s^{-1}$), stomatal conductance (g_s, mol H_2O $m^{-2}s^{-1}$), intrinsic water use efficiency (*iWUE*, µmol CO_2 mol H_2O^{-1}) and intracellular CO_2 concentration at 400 µmol mol^{-1} (operating c_i, µmol CO_2 $m^{-2}s^{-1}$) in cassava cultivars. Values represent mean ± SE. n = 8. Different letters represent statistically significant differences (P<0.05) among the cultivars.

Table 2. Time to reach 50% of light-saturated leaf carbon assimilation (T_{50A}, min), time to reach 90% of light-saturated leaf carbon assimilation (T_{90A}, min), cumulative CO_2 fixation in the first 5 min after photosynthesis induction (CCF, µmol CO_2), stomatal conductance at the beginning of photosynthesis induction (g_sT_0, mol H_2O $m^{-2}s^{-1}$), and time to reach 50% of maximum stomatal conductance (T_{50gs}, min) in cassava cultivars. Values represent mean ± SE. n = 6 except for cultivars TMS98/0505 and TMS97/2205 where n = 3. Different letters represent statistically significant differences (P<0.05) among the cultivars.

REFERENCES

Alene A, Abdoylaye T, Rusike J, Labarta R, Creamer B, del Río M, Ceballos H, Becerra L. 2018. Identifying crop research priorities based on potential economic and poverty reduction impacts: The case of cassava in Africa, Asia, and Latin America. *PLoS One* **13**(8): e0201803.

Allen M, Pearcy R. 2000. Stomatal behaviour and photosynthetic performance under dynamic light regimes in a seasonally dry tropical rain forest. *Oecologia* **122**: 470-478.

Barbour M, Bachmann S, Bansal U, Bariana H, Sharp P. 2016. Genetic control of mesophyll conductance in common wheat. *New Phytologist* **209**: 461-465.

Bernacchi CJ, Singsass EL, Pimentel C, Portis Jr AR, Long SP. 2001. Improved temperature responses functions for models of Rubisco-limited photosynthesis. *Plant, Cell & Environment* **24**(2): 253-260.

Bradford M. 1976. A rapid and sensitive method for the quantitation of microgram quantities of protein utilizing the principle of protein-dye binding. *Analytical Biochemistry* **72**(1-2): 248-254.

Carmo-Silva E, Andralojc PJ, Scales JC, Driever SM, Mead A, Lawson T, Raines C, Parry MA. 2017. Phenotyping of field-grown wheat in the UK highlights contribution of light response of photosynthesis and flag leaf longevity to grain yield. *Journal of Experimental Botany* **68**(13): 3473-3486.

Carmo-Silva E, Scales JC, Madgwick PJ, Parry MA. 2015. Optimizing Rubisco and its regulation for greater resource use efficiency. *Plant, Cell & Environment* **38**: 1817-1832.

Ceballos H, Iglesias C, Pérez J, Dixon A. 2004. Cassava breeding: opportunities and challenges. *Plant Molecular Biology* **56**(4): 503-516.

Ceballos H, Pérez J, Barandica O, Lenis JI, Morante N, Calle F, Pino L, Hershey C. 2016. Cassava breeding I: the value of breeding value. *Frontiers in Plant Science* **7**: 1227.

De Souza AP, Long SP. 2018. Toward improving photosynthesis in cassava: Characterizing photosynthetic limitations in four current African cultivars. *Food Energy Security* **7**(2): e00130.

De Souza AP, Massenburg LN, Jaiswal D, Cheng S, Shekar R, Long SP. 2017. Rooting for cassava: insights into photosynthesis and associated physiology as a route to improve yield potential. *New Phytologist* **213**(1): 50-65.

Driever SM, Lawson T, Andralojc PJ, Raines C, Parry MA. 2014. Natural variation in photostnthetic capacity, growth, and yield in 64 field-grown wheat genotypes. *Journal of Experimental Botany* **65**(17): 4959-4973.

El-Sharkawy MA. 2006. International research on cassava photosynthesis, productivity, eco-physiology, and responses to environmental stresses in the tropics *Photosynthetica* **44**(4): 481-512.

El-Sharkawy MA. 2016. Prospects of photosynthetic research for increasing agricultural productivity, with emphasis on the tropical C_4 Amaranthus and the cassava C_3-C_4 crops. *Photosynthetica* **54**: 161-184.

El-Sharkawy MA, Cock JH. 1990. Photosynthesis of Cassava (*Manihot esculenta*). *Experimental Agriculture* **26**: 325-340.

El-Sharkawy MA, Cock JH, Lynam J, Hernandez A, Cadavid LF. 1990. Relationships between biomass, root-yield and single-leaf photosynthesis in field-grown cassava. *Field Crops Research* **25**: 183-201.

El-Sharkawy MA, Lopez Y, Bernal L. 2008. Genotypic variations in activities of phosphoenolpyruvate carboxylase and correlations with leaf photosynthetic characteristics and crop productivity of cassava grown in low-land seasonally-dry tropics. *Photosynthetica* **46**: 238.

FAOSTAT 2019a. Most produced commodities. http://www.fao.org/faostat/en/#data/QC/: Food and Agriculture Organization of the United Nations.

FAOSTAT 2019b. Statistics of production. http://www.fao.org/faostat/en/#data/QC/visualize: Food and Agriculture Organization of the United Nations.

Feller U, Crafts-Brandner S, Salvucci ME. 1998. Moderately high temperatures inhibit ribulose-1, 5-bisphosphate carboxylase/oxygenase (Rubisco) activase-mediated activation of Rubisco. *Plant Physiology* **116**(2): 539-546.

Fisher R, Rees D, Sayre K, Lu Z-M, Condon A, Saavendra A. 1998. Wheat yield progress associated with higher stomatal conductance and photosynthetic rate, and cooler canopies. *Crop Science* **38**: 1467-1475.

Flexas J, Diaz-Espejo A, Conesa MA, Coopman R, Douthe C, Gago J, Gallé A, Galmés J, Medrano H, Ribas-Carbó M, et al. 2016. Mesophyll conductance to CO_2 and Rubisco as targets for improving intrinsic water use efficiency in C_3 plants. *Plant, Cell & Environment* **39**: 965-982.

Flexas J, Ribas-Carbó M, Diaz-Espejo A, Galmés J, Medrano H. 2008. Mesophyll conductance to CO_2: current knowledge and future prospects. *Plant, Cell & Environment* **31**(5): 602-621.

Flexas J, Ribas-Carbó M, Hanson D, Bota J, Otto B, Cifre J, McDowell N, Medrano H, Kaldenhoff R. 2006. Tobacco aquaporin NtAQP1 is involved in mesophyll conductance to CO_2 *in vivo*. *The Plant Journal* **48**(3): 427-439.

Glowacka K, Kromdijk J, Kucera K, Xie J, Cavanagh AP, Leonelli L, Leakey ADB, Ort D, Niyogi KK, Long SP. 2018. Photosystem II Subunit S overexpression increases the efficiency of water use in a field-grown crop. *Nature Communications* **9**: 868.

Grassi G, Magnani F. 2005. Stomatal, mesophyll conductance and biochemical limitations to photosynthesis as afffected by drought and leaf onthogeny in ash and oak trees. *Plant, Cell & Environment* **28**: 834-849.

Gu J, Yin X, Stomph T-J, Wang H, Struick P. 2012. Physiological basis of genetic variation in leaf photosynthesis among rice (*Oryza sativa* L.) introgression lines under drought and well-watered conditions. *Journal of Experimental Botany* **63**(14): 5137-5153.

Hammond E, Andrews T, Mott K, Woodrow I. 1998. Regulation of Rubisco activation in antisense plants of tobacco containing reduced levels of Rubisco activase. *The Plant Journal* **14**: 101-110.

Hanba Y, Shibasaka M, Hayashi Y, Hayakawa T, Kasamo K, Terashima I, Katsuhara M. 2004. Overexpression of the barley aquaporin HvPIP2;1 increases internal CO_2 conductance and CO_2 assimilation in the leaves of transgenic rice plants. *Plant and Cell Physiology* **45**(5): 521-529.

Harley P, Loreto F, Di Marco G, Sharkey TD. 1992. Theoretical considerations when estimating mesophyll conductance to CO_2 flux by analysis of the response of photosynthesis to CO_2. *Plant Physiology* **98**: 1429-1436.

Henry G, Grafffham A, Westby A, Vilpoux O, Ospina M, Titapiwatanakun B, Taylor D, Phillips T. 2004. *Procedings of the validation forum on the global cassava development strategy*. Rome: FAO and IDAF.

Ihemere U, Arias-Garzon D, Lawrence S, Sayre R. 2006. Genetic modification of cassava for enhanced starch production. *Plant Biotechnol Journal* **4**(4): 453-465.

Jahan E, Amthor J, Farquhar GD, Trethowan R, Barbour M. 2014. Variation in mesophyll conductance among Australian wheat genotypes. *Functional Plant Biology* **41**: 568-580.

Jaikumar N, Snapp S, Sharkey TD. 2013. Life history and resource acquisition: photosynthetic traits in selected accessions of three perennial cereal species compared with annual wheat and rye. *American Journal of Botany* **100**: 2468-2477.

Jonik C, Sonnewald U, Hajirezaei M-R, Flugge U-I, Ludewig F. 2012. Simultaneous boosting of source and sink capacities doubles tuber starch yield of potato plants. *Plant Biotechnology Journal* **10**(9): 1088-1098.

Kleih U, Phillips D, Wordey M, Komlaga G. 2013. Cassava market and value chain analysis: Ghana case study.

Koester RP, Skoneczka JA, Cary TR, Diers BW, Ainsworth EA. 2014. Historical gains in soybean (Glycine max Merr.) seed yield are driven by linear increases in light interception, energy conversion, and partitioning efficiencies. *J Exp Bot* **65**(12): 3311-3321.

Kromdijk J, Glowacka K, L L, Gabilly S, Iwai M, Niyogi KK, Long S. 2016. Improving photosynthesis and crop productivity by accelerating recovery from photoprotection. *Science* **354**: 857-861.

Lawson T, Blatt M. 2014. Stomatal size, speed, and responsiveness impact on photosynthesis and water use efficiency. *Plant Physiology* **164**: 1556-1570.

Lebot V. 2009. *Tropical roots and tuber crops: cassava, sweet potato, yams and aroids*. Reading, UK: UK by MPG Biddles Ltd.

Lefebvre S, Lawson T, Fryer M, Zakhleniuk O, Lloyd J, Raines C. 2005. Increased sedoheptulose-1, 7-bisphosphatase activity in transgenic tobacco plants stimulates photosynthesis and growth from an early stage in development. *Plant Physiology* **138**: 451-460.

Long SP, Bernacchi CJ. 2003. Gas exchange measurements, what can they tell us about the underlying limitations of photosynthesis? Procedures and sources of error. *Journal of Experimental Botany* **54**(392): 2393-2401.

Long SP, Zhu X-G, Naidu SL, Ort DR. 2006. Can improvement in photosynthesis increase crop yields? *Plant, Cell & Environment* **29**: 305-330.

Masumoto C, Ishii T, Hatanaka T, Uchida N. 2005. Mechanism of high photosynthetic capacity in BC_2F_4 lines derived from a cross between *Oryza sativa* and wild relatives *O.rufipogon*. *Plant Production Science* **8**: 539-545.

Mate C, von Caemmerer S, Evans JR, Hudson G, Andrews T. 1996. The relationship between CO_2-assimilation rate, Rubisco carbamylation and Rubisco activase content in activase-deficient transgenic tobacco suggests a simple model of activase action. *Planta* **198**(4): 604-613.

McAusland L, Vialet-Chabrand S, Davey P, Baker N, Brendel O, Lawson T. 2016. Effects of kinetics of light-induced stomatal responses on photosynthesis and water-use efficiency. *New Phytologist* **211**(4): 1209-1220.

McMurtrie RE, Wang YP. 1993. Mathematical models of the photosynthetic response of tree stands to rising CO_2 concentrations and temperature. *Plant, Cell & Environment* **16**: 1-13.

Mott K, Woodrow I. 2000. Modeling the role of Rubisco activase in limiting non-steady-state photosynthesis. *Journal of Experimental Botany* **51**: 399-406.

Moualeu-Ngangue D, Chen T-W, Stutzel H. 2017. A new method to estimate photosynthetic parameters through net assimilation rate-intracellular space CO_2 concentration (A-C_i) curve and chlorophyll fluorescence measurements. *New Phytologist* **213**: 1543-1554.

Nassar N, Ortiz R. 2010. Breeding cassava. *Scientifican American* **302**(5): 78-84.

Orr D, Alcântara A, Kapralov MV, Andralojc PJ, Carmo-Silva E, Parry MA. 2016. Surveying Rubisco diversity and temperature response to improve crop photosynthetic efficiency. *Plant Physiology* **172**: 707-717.

Papanatsiou M, Petersen J, Henderson L, Wang J, Christie J, Blatt M. 2019. Optogenetic manipulation of stomatal kinetics improves carbon assimilation, water use, and growth. *Science* **29**: 1456-1459.

Parry M, Andralojc PJ, Parmar S, Keys AJ, Habash D, Paul M, Alred R, Quick W, Servaites J. 1997. Regulation of Rubisco by inhibitors in the light. *Plant, Cell & Environment* **20**: 528-534.

Parry MA, Madgwick PJ, Carvalho J, Andralojc PJ. 2007. Prospects for increasing photosynthesis by overcoming the limitations of Rubisco. *Journal of Agricultural Science* **145**: 31-43.

Pearcy R. 1990. Sunflecks and photosynthesis in plant canopies. *Annual Review of Plant Physiology and Plant Molecular Biology* **41**: 421-453.

Perdomo J, Sales C, Carmo-Silva E 2018. Quantification of photosynthetic enzymes in leaf extracts by immunoblotting. In: Covshoff S ed. *Photosynthesis. Methods in Molecular Biology*. New York, NY: Humana Press, 215-227.

Reynolds M, Balota M, Delgado M, Amani I, Fischer RA. 1994. Physiological and morphological traits associated with spring wheat yield under hot, irrigated conditions. *Functional Plant Biology* **21**: 717-730.

Rosenthal DM, Slattery RA, Miller RE, Grennan AK, Cavagnaro TR, Fauquet CM, Gleadow RM, Ort DR. 2012. Cassava about-FACE: Greater than expected yield

stimulation of cassava (*Manihot esculenta*) by future CO_2 levels. *Global Change Biology* **18**(8): 2661-2675.

Sharkey T. 1985. Photosynthesis in intact leaves of C_3 plants: physics, physiology, and rate limitations. *Botanical Review* **51**: 53-105.

Sharkey TD, Bernacchi CJ, Farquhar GD, Singsaas EL. 2007. Fitting photosynthetic carbon dioxide response curves for C_3 leaves. *Plant, Cell & Environment* **30**(9): 1035-1040.

Sharwood R, Sonowane B, Ghannoum O, Whitney S. 2016. Improved analysis of C_4 and C_3 photosynthesis via refined in vitro assays of their carbon fixation biochemistry. *Journal of Experimental Botany* **67**: 3137-3148.

Simkin AJ, López-Calcagno P, Raines C. 2019. Feeding the world: improving photosynthetic efficiency for sustainable crop production. *Journal of Experimental Botany* **70**(4): 1119-1140.

Soleh M, Tanaka Y, Nomoto Y, Iwahashi Y, Nakashima K, Fukuda Y, Long SP, Shiraiwa T. 2016. Factors underlying genotypic differences in the induction of photosynthesis in soybean [*Glycine max* (L.) Merr.]. *Plant, Cell & Environment* **39**: 685-693.

Sonnewald U, Fernie AR. 2018. Next-generation strategies for understanding and influencing source–sink relations in crop plants. *Current Opinion in Plant Biology* **43**: 63-70.

South PF, Cavanagh AP, Liu HW, Ort D. 2019. Synthetic glycolate metabolism pathways stimulate crop growth and productivity in the field. *Science* **363**: eaat9077.

Tadele Z. 2018. African orphan crops under abiotic stresses: challenges and opportunities. *Scientifica* **2018**: 1451894.

Taylor S, Long SP. 2017. Slow induction of photosynthesis on shade to sun transitions in wheat may cost at least 21% of productivity. *Philosophical Transactions of the Royal Society B* **372**: 20160543.

Theobald J, Mitchell R, Parry MA, Lawlor D. 1998. Estimating the excess investiment in ribulose-1,5-bisphosphate carboxylase/oxygenase in leaves of spring wheat grown under elevated CO_2. *Plant Physiology* **118**: 945-955.

Uchechykwu-Agua A, Caleb O, Opara U. 2015. Postharvest handling and storage of fresh cassava root and products: a review. *Food and Bioprocess Technology* **8**(4): 729-748.

United Nations. 2017. World population prospects: the 2017 revision, key findings and advance tables. Working Papaer no ESA/P/WP/248, New York: United Nations.

van Ittersum M, van Bussel L, Wolf J, Grassini P, van Wart J, Guilpart N, Claessens L, Groot H, Wiebe K, Mason-D'Croz D, et al. 2016. Can sub-Saharan Africa feed itself? *PNAS* **113**(52): 14964-14969.

Vialet-Chabrand S, Matthews J, McAusland L, Blatt M, Griffiths H, Lawson T. 2017. Temporal dynamics of stomatal behavior" modelling and inplications for photosynthesis and water use. *Plant Physiology* **174**(2): 603-613.

von Caemmerer S. 2000. *Biochemical models of leaf photosynthesis*. Collingwood, Australia: CSIRO Publishing.

Way D, Pearcy R. 2012. Sunflecks in trees and forests: from photosynthetic physiology to global change biology. *Tree Physiology* **32**(9): 1066-1081.

Whitney S, Houtz R, Alonso H. 2011. Advancing our understanding and capacity to engineer nature's CO_2-sequestring enzyme, Rubisco. *Plant Physiology* **155**: 27-35.

Wintermans J, de Mots A. 1965. Spectrophotometric characteristics of chlorophylls *a* and *b* and their pheophytins in ethanol. *Biochimica et Biophysica Acta* **109**: 448-453.

World Bank. 2017. Atlas of sustainable development goals 2017: world development indicators. Washington DC: World Bank, License: CC BY 3.0 IGO.

Wullschleger SD. 1993. Biochemical limitations to carbon assimilation in C_3 plants - a retrospective analysis of the A/C_i curves from 109 species. *Journal of Experimental Botany* **44**: 907-920.

Xiong D, Douthe C, Flexas J. 2018. Differential coordination of stomatal conductance, mesophyll conductance, and leaf hydraulic conductance in response to changing light across species. *Plant, Cell & Environment* **41**: 436-450.

Yamori W, Masumoto C, Fukayama H, Makino A. 2012. Rubisco activase is a key regulator of non-steady-state photosynthesis at any leaf temperature and, to a lesser extend, of steady-state photosynthesis at high temperature. *The Plant Journal* **71**: 871-880.

Yang J, Preiser A, Li Z, Weise S, Sharkey TD. 2016. Triose phosphate use limitation of photosynthesis: short-term and long-term effects. *Planta* **243**(3): 687-698.

Zhu X-G, de Sturler E, Long SP. 2007. Optimizing the distribution of resources between enzymes of carbon metabolism can dramatically increase photosynthetic rate: A numerical simulation using an evolutionary algorithm. *Plant Physiology* **145**(2): 513-526.

Zhu XG, Long SP, Ort DR. 2010. Improving photosynthetic efficiency for greater yield. *Annu Rev Plant Biol* **61**: 235-261.

Zhu XG, Ort DR, Whitmarsh J, Long SP. 2004. The slow reversibility of photosystem II thermal energy dissipation on transfer from high to low light may cause large losses in

carbon gain by crop canopies: a theoretical analysis. *Journal of Experimental Botany* **55**(400): 1167-1175.

Zhu XG, Wang Y, Ort D, Long SP. 2013. e-photosynthesis: a comprehensive dynamic mechanistic model of C_3 photosynthesis: from light capture to sucrose synthesis. *Plant, Cell & Environment* **36**(9): 1711-1727.

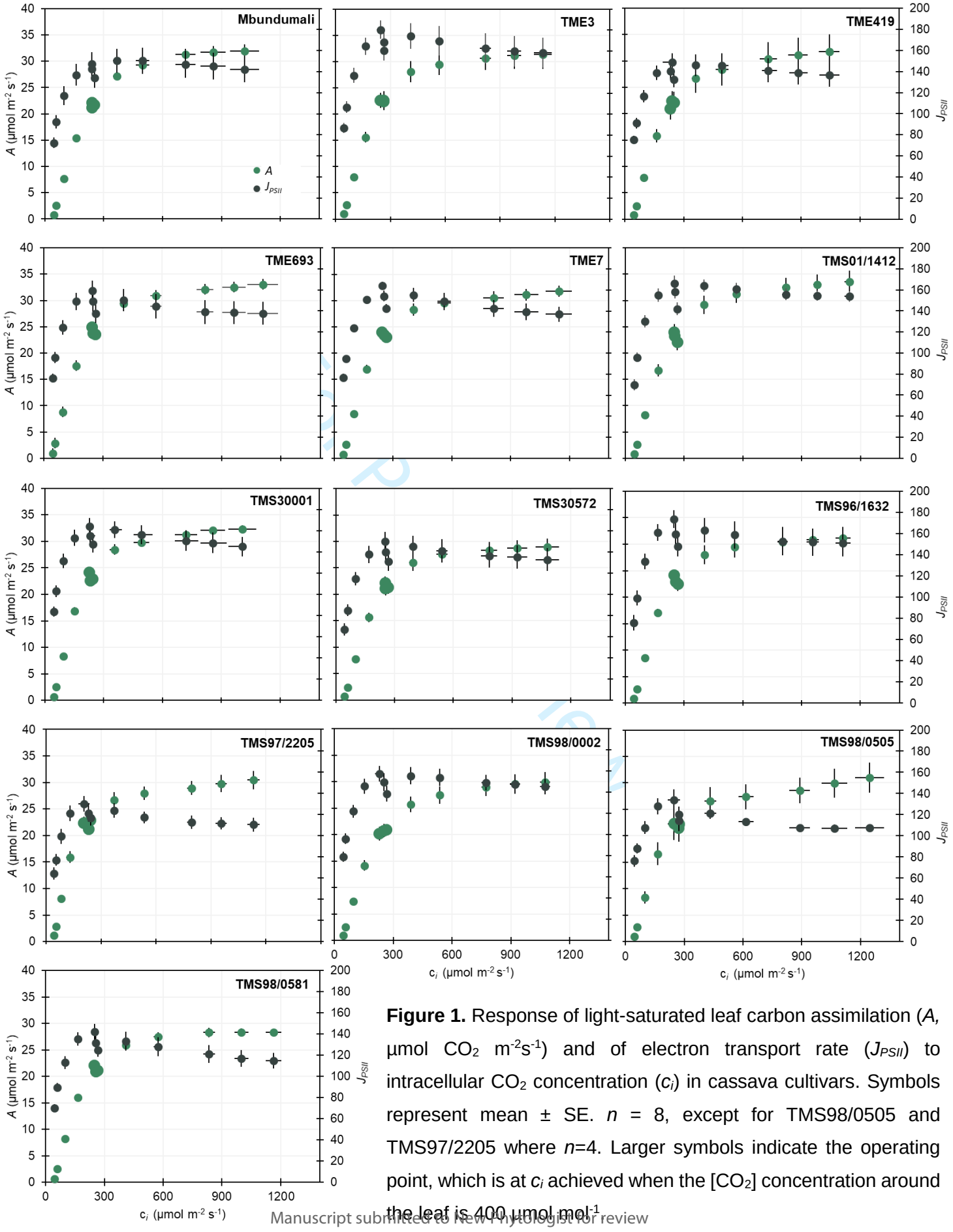

Figure 1. Response of light-saturated leaf carbon assimilation (*A*, µmol CO_2 $m^{-2}s^{-1}$) and of electron transport rate (J_{PSII}) to intracellular CO_2 concentration (c_i) in cassava cultivars. Symbols represent mean ± SE. *n* = 8, except for TMS98/0505 and TMS97/2205 where *n*=4. Larger symbols indicate the operating point, which is at c_i achieved when the [CO_2] concentration around the leaf is 400 µmol mol^{-1}.

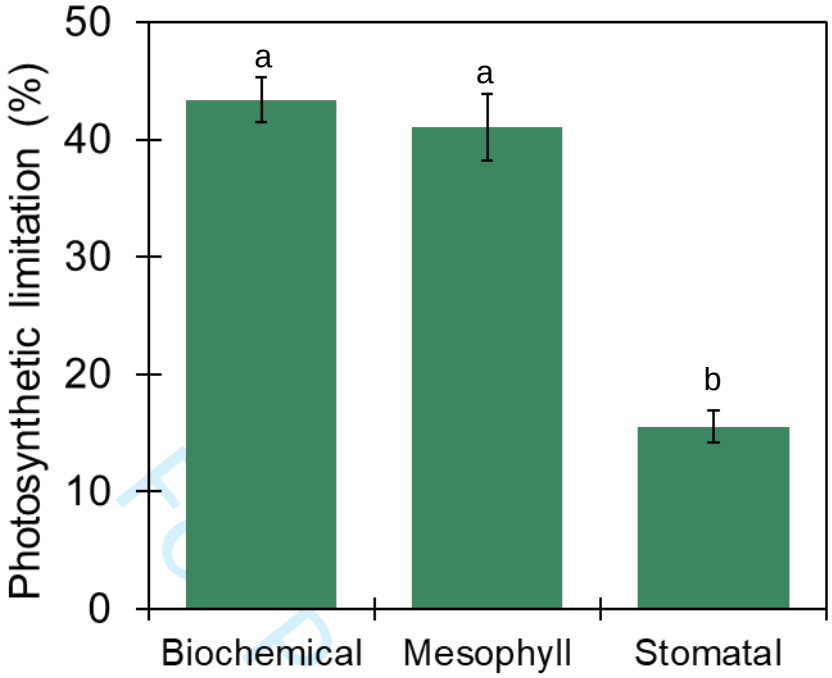

Figure 2. Relative biochemical, mesophyll and stomatal limitations under steady state in cassava. The total limitation is equal to 100%. Bars represent mean ± SE of all cultivars. Different letters represent statistically significant differences (P<0.05) between different limitations.

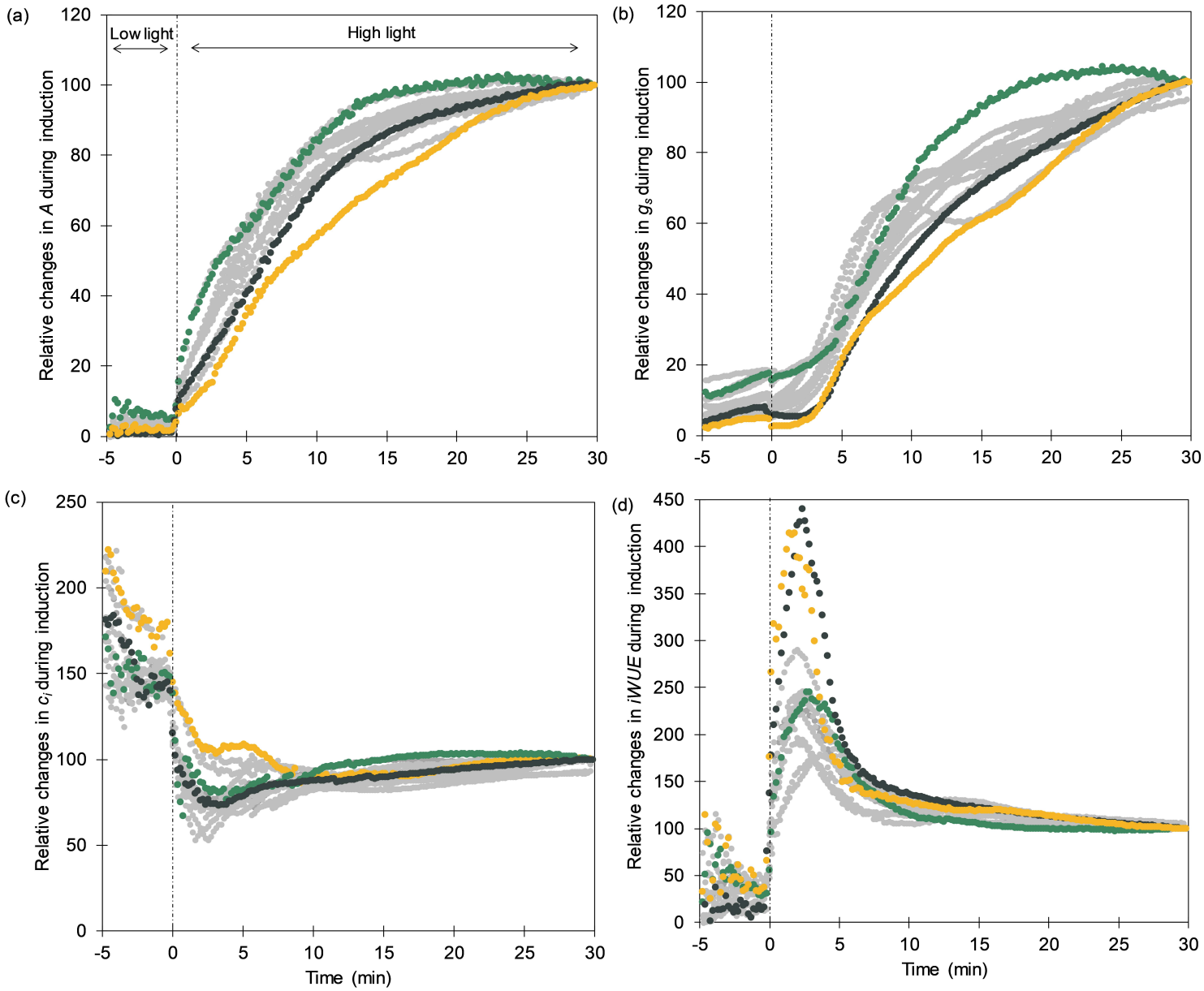

Figure 3. Changes in leaf carbon assimilation (A, μmol CO_2 $m^{-2}s^{-1}$) **(a)**, stomatal conductance (g_s, mol H_2O $m^{-2}s^{-1}$) **(b)**, internal CO_2 concentration (c_i, μmol CO_2 $m^{-2}s^{-1}$) **(c)**, and intrinsic water use efficiency (*i*WUE, μmol CO_2 mol H_2O^{-1}) **(d)** in cassava cultivars during photosynthesis induction. Relative values were calculated as the percentage of the value obtained after 30 minutes under high light. During low light and high light phase, the light was 50 μmol $m^{-2}s^{-1}$ and 1500 μmol $m^{-2}s^{-1}$ PPFD, respectively. Colored lines indicate cultivars with contrasting responses (TME693 and TMS98/0505) and the cultivar TME7. Data represent mean. n = 6 except for genotypes TMS98/0505 and TMS97/2205 where n = 3.

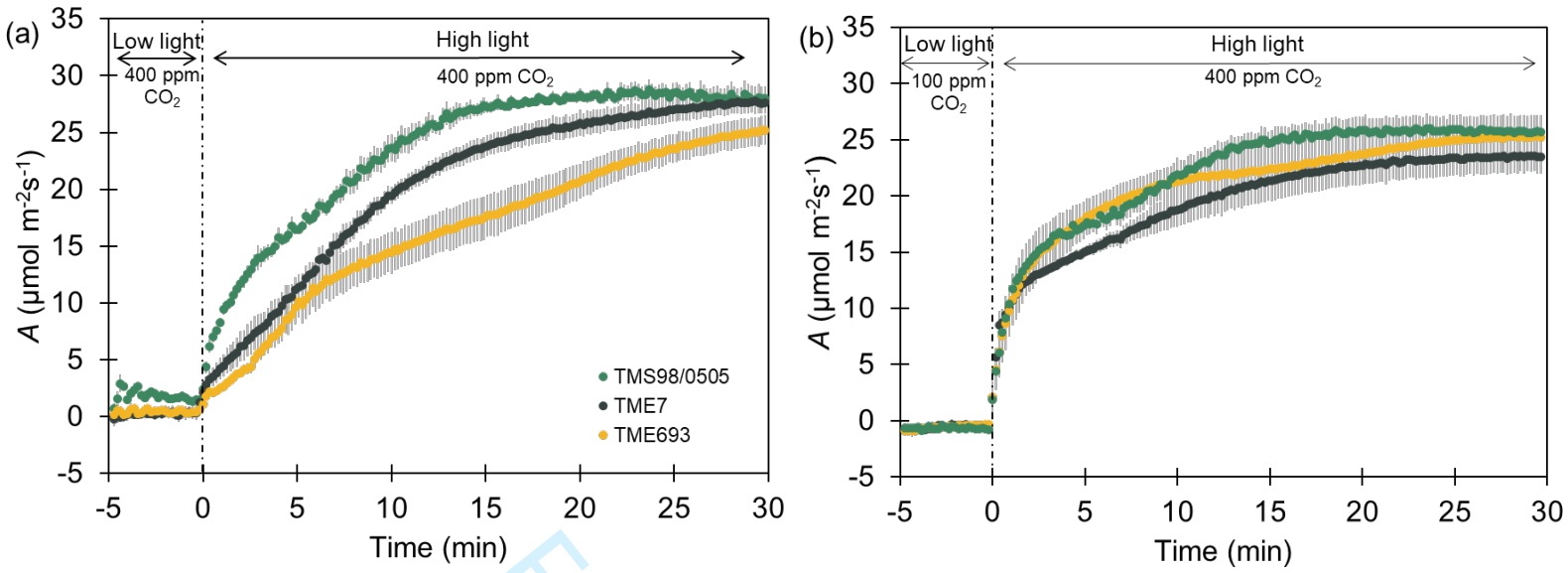

(c)

[CO_2] during low light	Cultivar	T_{50A}	T_{90A}	CCF	g_{sT0}
400ppm	TME693	10.6 ± 1.39a	21.18 ± 1.13a	121.52 ± 27.25c	0.005 ± 0.004c
	TME7	6.42 ± 0.53b	17.02 ± 1.64a	200.84 ± 35.45b	0.019 ± 0.003b
	TMS98/0505	3.1 ± 0.23c	11.57 ± 0.69b	348.92 ± 16.08a	0.047 ± 0.003a
100pm	TME693	0.82 ± 0.19a	10.62 ± 3.3a	332.24 ± 58.65a	0.118 ± 0.029a
	TME7	2.12 ± 0.62a	15.47 ± 1.8a	344.73 ± 14.48a	0.134 ± 0.016a
	TMS98/0505	1.22 ± 0.44a	17.13 ± 3.02a	380.92 ± 49a	0.162 ± 0.023a

Figure 4. Leaf carbon assimilation (A, µmol CO_2 $m^{-2}s^{-1}$) during induction with CO_2 concentration during low light phase set at 400 ppm **(a)** or 100 ppm **(b)**. During the high light phase of the induction, CO_2 concentration was maintained at 400 ppm in both measurements. Comparison among cultivars related to time to reach 50% of light-saturated leaf carbon assimilation (T_{50A}, min), time to reach 90% of light-saturated leaf carbon assimilation (T_{90A}, min), cumulative CO_2 concentration in the first 5 min after photosynthesis induction (CCF, µmol CO_2), and stomatal conductance at the beginning of photosynthesis induction (g_{sT0}, mol H_2O $m^{-2}s^{-1}$) in both CO_2 concentrations during low light phase **(c)**. Values represent mean ± SE. n=6 for TME693 and TME7; n=3 for TMS98/0505. Different letters represent statistically significant differences (P<0.05) among the cultivars.

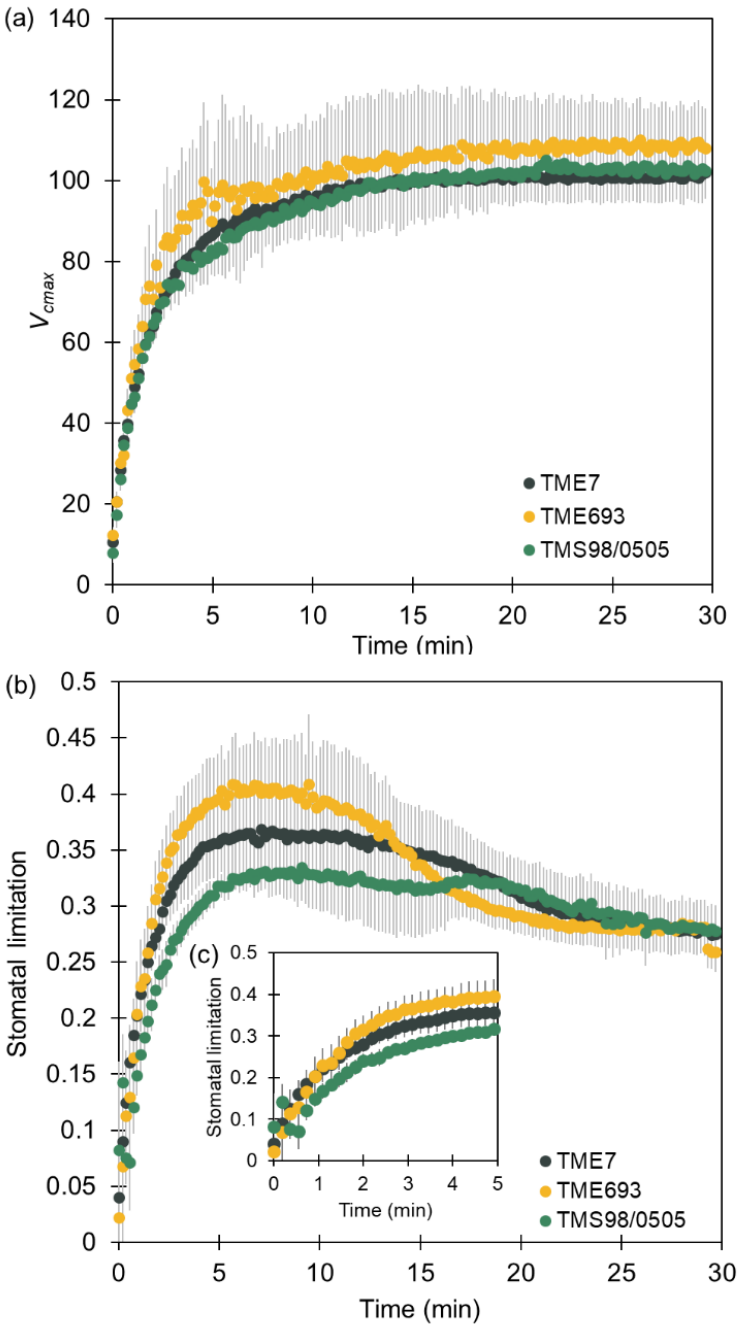

Figure 5. Maximum carboxylation rate by Rubisco (V_{cmax}, μmol $m^{-2}s^{-1}$) **(a)** and stomatal limitation during photosynthesis induction **(b,c)** in three cassava cultivars. Data represent mean ± SE. *n*=3-4.

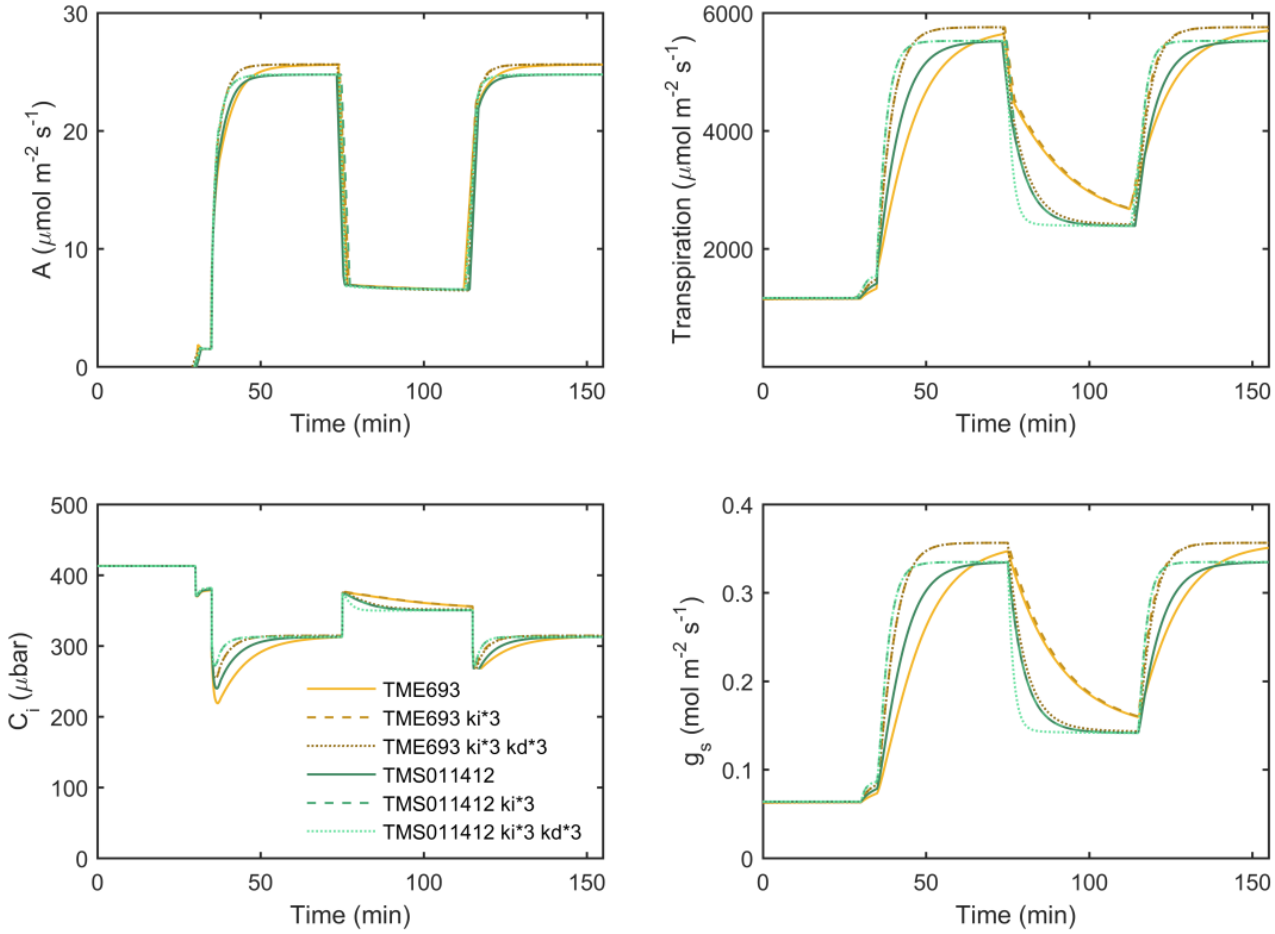

Figure 6. Model simulated carbon assimilation rate (*A*), transpiration rate (*T*), intercellular CO_2 concentration (c_i) and stomata conductance (g_s) of cultivars TME693 and TMS01/1412. Light in PPFD input is: 0 μmol m^{-2} s^{-1} in the first 30 min, 50 μmol m^{-2} s^{-1} from 30 min to 35 min, 1500μmol m^{-2} s^{-1} from 35 min to 75 min; 150μmol m^{-2} s^{-1} from 75 min to 115 min; and 1500 μmol m^{-2} s^{-1} from 115 min to 155 min. Name of the cultivars followed by k_i*3 or k_i*3 k_d*3 represents the simulation considering the acceleration by three time of the stomata opening and stomata opening and closure, respectively.

Table 1. Light-saturated leaf carbon assimilation (A_{sat}, µmol CO_2 $m^{-2}s^{-1}$), apparent maximum carboxylation rate by Rubisco (V_{cmax}, µmol $m^{-2}s^{-1}$), maximum carboxylation rate by Rubisco estimated based on partial pressure of CO_2 inside the chloroplast ($V_{cmax, Cc}$, µmol $m^{-2}s^{-1}$), regeneration of ribulose-1,5-bisphosphate represented by electron transport rate (J_{max}, µmol $m^{-2}s^{-1}$), triose phosphate utilization ($V_{TPU,}$ µmol $m^{-2}s^{-1}$), stomatal conductance (g_s, mol H_2O $m^{-2}s^{-1}$), intrinsic water use efficiency (*iWUE*, µmol CO_2 mol H_2O^{-1}) and intracellular CO_2 concentration at 400 µmol mol^{-1} (operating c_i, µmol CO_2 $m^{-2}s^{-1}$) in cassava cultivars. Values represent mean ± SE. n = 8. Different letters represent statistically significant differences (P<0.05) among the cultivars.

Cultivar	A_{sat}	V_{cmax}	$V_{cmax,Cc}$	J_{max}	V_{TPU}	g_s	*iWUE*	operating c_i
Mbundumali	20.32 ± 1.05b	100.12 ± 3.96b	124.81 ± 12.47ab	169.41 ± 6.01a	11.03 ± 0.43ab	0.28 ± 0.02abc	81.63 ± 5.84ab	244.1 ± 9.45ab
TME3	21.49 ± 1.78abcd	101.83 ± 10.75ab	156.73 ± 8.51a	165.39 ± 14.52ab	10.85 ± 0.89ab	0.34 ± 0.02a	71.66 ± 7.15ab	257.43 ± 11.08ab
TME419	22.17 ± 1.36abcd	118.18 ± 6.90a	128.28 ± 5.98b	183.86 ± 14.78a	11.65 ± 0.81ab	0.27 ± 0.02bc	83.07 ± 4.48ab	241.21 ± 7.69ab
TME693	23.22 ± 1.27abcd	110.29 ± 7.42ab	133.19 ± 13.71ab	171.3 ± 11.08ab	11.43 ± 0.7ab	0.33 ± 0.02abc	75.41 ± 4.01ab	252.96 ± 6.77ab
TME7	24.61 ± 1.60ac	104.82 ± 2.72ab	140.44 ± 8.79b	163.45 ± 7.47ab	10.9 ± 0.36a	0.34 ± 0.03abc	74.22 ± 4.88ab	254.91 ± 7.70ab
TMS01/1412	24.81 ± 1.22a	113.48 ± 3.83a	135.62 ± 6.05ab	175.88 ± 11.59a	11.46 ± 0.68a	0.32 ± 0.01a	73.35 ± 4.85b	255.77 ± 7.73ab
TMS30001	22.95 ± 1.27abcd	117.16 ± 6.87a	136.24 ± 7.21ab	169.67 ± 5.73a	11.13 ± 0.26a	0.28 ± 0.02c	86.57 ± 4.52ab	235.19 ± 7.33b
TMS30572	20.81 ± 0.95bd	95.24 ± 4.83ab	120.63 ± 9.86b	154.5 ± 10.56ab	9.97 ± 0.50ab	0.32 ± 0.04abc	72.92 ± 6.13ab	258.15 ± 9.35ab
TMS96/1632	24.21 ± 1.23ac	102.65 ± 6.75ab	141.65 ± 9.45ab	163.24 ± 14.20ab	10.83 ± 0.70b	0.33 ± 0.01a	71.49 ± 3.38b	258.63 ± 5.12a
TMS97/2205	22.12 ± 0.37b	100.33 ± 2.70ab	122.47 ± 10.8b	157.68 ± 7.50ab	10.77 ± 0.51ab	0.25 ± 0.02c	93.48 ± 6.91a	226.83 ± 10.84b
TMS98/0002	21.92 ± 1.26abcd	96.28 ± 2.23b	119.68 ± 8.7b	149.36 ± 10.15ab	10.5 ± 0.69ab	0.29 ± 0.03abc	78.96 ± 8.99ab	249.02 ± 13.49ab
TMS98/0505	21.49 ± 0.62bc	97.06 ± 11.21ab	132.68 ± 9.55ab	161.15 ± 13.25ab	10.45 ± 0.70ab	0.3 ± 0.01abc	78.7 ± 1.32ab	250.41 ± 2.23ab
TMS98/0581	23.11 ± 1.12abcd	99.33 ± 4.36ab	138.67 ± 7.6ab	148.69 ± 4.63b	9.88 ± 0.24b	0.31 ± 0.02abc	73.47 ± 5.31ab	257.31 ± 8.53ab

Table 2. Time to reach 50% of light-saturated leaf carbon assimilation (T_{50A}, min), time to reach 90% of light-saturated leaf carbon assimilation (T_{90A}, min), cumulative CO_2 fixation in the first 5 min after photosynthesis induction (CCF, µmol CO_2), stomatal conductance at the beginning of photosynthesis induction (g_sT_0, mol H_2O $m^{-2}s^{-1}$), and time to reach 50% of maximum stomatal conductance (T_{50gs}, min) in cassava cultivars. Values represent mean ± SE. *n* = 6 except for cultivars TMS98/0505 and TMS97/2205 where *n* = 3. Different letters represent statistically significant differences (P<0.05) among the cultivars.

Cultivar	T_{50A}	T_{90A}	CCF	g_sT_0	T_{50gs}
Mbundumali	4.2 ± 0.3d	13.8 ± 0.6bcd	272 ± 20.7abcde	0.032 ± 0.006abcd	8.08 ± 0.52abc
TME3	6.1 ± 0.4bc	15.5 ± 1.2bcd	187 ± 22.7def	0.016 ± 0.003de	7.7 ± 0.58abc
TME419	4.6 ± 0.7cd	14 ± 1.5bcd	291 ± 24.3abc	0.027 ± 0.006abcde	7.38 ± 1.20bc
TME693	10.6 ± 1.4a	21.2 ± 1.1a	122 ± 27.2f	0.005 ± 0.004e	9.48 ± 2.11ab
TME7	6.4 ± 0.5b	17.0 ± 1.6abc	201 ± 35.4cdef	0.019 ± 0.003cde	10.58 ± 1.43a
TMS01/1412	3.5 ± 0.5d	17.1 ± 1.5abc	179 ± 31.6ef	0.025 ± 0.006bcde	5.75 ± 0.96c
TMS30001	4.1 ± 0.5d	17.1 ± 2.2abc	280 ± 46.2abcd	0.028 ± 0.006abcde	6.21 ± 0.55c
TMS30572	5.1 ± 0.7bcd	13.3 ± 1.6cd	262 ± 40.5abcde	0.020 ± 0.005cde	7.67 ± 0.55abc
TMS96/1632	4.5 ± 0.8cd	17.8 ± 1.3ab	276 ± 45.8abcde	0.045 ± 0.008ab	10.33 ± 1.32ab
TMS97/2205	3.1 ± 1.0d	11.3 ± 0.5d	333 ± 46.1ab	0.054 ± 0.013a	7.4 ± 0.92abc
TMS98/0002	4.0 ± 0.7d	16.4 ± 2.2bcd	279 ± 41.2abcd	0.032 ± 0.013abcd	5.73 ± 0.67c
TMS98/0505	3.1 ± 0.2d	11.6 ± 0.7d	349 ± 16.1a	0.047 ± 0.003abc	7.18 ± 1.78abc
TMS98/0581	4.2 ± 0.6d	17.6 ± 1.6ab	226 ± 33.9bcde	0.034 ± 0.015abcd	7.36 ± 0.69bc